

OPTIMAL HOLONOMIC QUANTUM GATES

ANTTI O. NISKANEN

*Materials Physics Laboratory, Helsinki University of Technology,
P. O. Box 2200 (Technical Physics), FIN-02015 HUT, Finland*

MIKIO NAKAHARA*

*Department of Physics, Kinki University
Higashi-Osaka 577-8502, Japan*

MARTTI M. SALOMAA

*Materials Physics Laboratory, Helsinki University of Technology,
P. O. Box 2200 (Technical Physics), FIN-02015 HUT, Finland*

Received September 30, 2002

We study the construction of holonomy loops numerically in a realization-independent model of holonomic quantum computation. The aim is twofold. First, we present our technique of finding the suitable loop in the control manifold for any one-qubit and two-qubit unitary gates. Second, we develop the formalism further and add a penalty term for the length of the loop, thereby aiming to minimize the execution time for the quantum computation. Our method provides a general means by which holonomy loops can be realized in an experimental setup. Since holonomic quantum computation is adiabatic, optimizing with respect to the length of the loop may prove crucial.

Keywords: quantum geometric and topological computations, numerical optimization

Communicated by: R Cleve

1. Introduction

We study the implementation of a quantum computer numerically using so-called non-Abelian holonomies. Holonomic quantum computation (HQC) was suggested by Zanardi and Rasetti in Ref. [1] and further developed, e.g., in Refs. [2, 3, 4, 5, 6, 7, 8]. In order to build a working quantum computer of N qubits, one has to be able to produce any unitary operations in $U(2^N)$, i.e. time-evolutions, on the qubits. In holonomic quantum computation, these operations are achieved by selecting a degenerate qubit system and allowing for an adiabatic time-development that does not change the degeneracy structure. Even though the Hamiltonian in this subspace is completely trivial, it turns out that a non-Abelian and irreducible gauge potential appears, using which any unitary evolution can be carried out. As the word holonomy itself suggests, we drive the system around loops in the control-parameter space (or

*Also at the Materials Physics Laboratory, Helsinki University of Technology, P. O. Box 2200 (Technical Physics), FIN-02015 HUT, Finland.

manifold) and after each loop there is a nontrivial change in the state of the system. This is a generalization of the famous Berry phase [9] to a degenerate system.

This paper is organized as follows. In Section 2 we first review the concept of non-Abelian holonomy. Then in Section 3 we introduce our realization-independent model. Namely, we consider the general setting for non-Abelian holonomy and unitary gate construction in a three-state system. This part applies to a much wider class of research topics in modern physics than just quantum computation. Many physical systems may be suitable for the actual implementation of this model. Section 4 is the main part of the work. There we first consider the generic algorithm for numerically finding implementations of holonomic quantum gates. We have previously studied the computational construction of holonomic quantum gates in Ref. [10]. There we limited our attention, however, to the solution of the inversion problem itself; we showed that one can numerically find a holonomy loop corresponding to a desired gate. Here we further extend the concept to actually optimizing with respect to the length of the path. We find some new and more efficient implementations of holonomic quantum gates. Because holonomic quantum computation is adiabatic and hence time-consuming, it is important to optimize the construction of quantum gates. We argue that our optimization method could also be extended to dynamical quantum computation. Section 5 is devoted to discussion.

2. Non-Abelian Holonomy

We briefly outline the concept of non-Abelian holonomy associated with adiabatic change of control parameters. This is necessary not only to establish notation conventions but also to rectify certain confusion appearing in the literature on the definition of the holonomy operator. The concept was first introduced by Wilczek and Zee in Ref. [11]. Other excellent references are Zee [12] and Mostafazadeh [13].

Let us consider a family of Hamiltonians $\{H_\lambda\}$ parameterized by $\lambda \in M$, where M is a manifold called the control manifold. The local coordinate of λ is denoted by λ^i ($1 \leq i \leq m = \dim M$). We assume that there are only a finite number of eigenvalues $\varepsilon_k(\lambda)$ ($1 \leq k \leq R$) for an arbitrary point λ of M and that no level crossings take place through all of M . The eigenvalue $\varepsilon_k(\lambda)$ is assumed to be g_k -fold degenerate independently of λ . This degenerate subspace will be denoted by $\mathcal{H}_k(\lambda)$. Then the Hamiltonian is expressed as an $N \times N$ hermitian matrix, where $N = \sum_{k=1}^R g_k$.

Let us denote the orthonormal basis vectors of $\mathcal{H}_k(\lambda)$ as $\{|k\alpha; \lambda\rangle\}$;

$$H_\lambda |k\alpha; \lambda\rangle = \varepsilon_k(\lambda) |k\alpha; \lambda\rangle, \quad \langle j\alpha; \lambda | k\beta; \lambda \rangle = \delta_{jk} \delta_{\alpha\beta}. \quad (1)$$

Note that there are $U(g_k)$ degrees of freedom in choosing the set of basis vectors $\{|k\alpha; \lambda\rangle\}$.

Suppose the control parameter λ is varied continuously over M . It is assumed that the variation is so slow that the adiabaticity condition is fulfilled, i.e., transitions between the different energy levels are negligible. We will be concerned with a particular subspace, the ground state \mathcal{H}_1 , for example. We will drop the index $k = 1$ hereafter to simplify the notation. Let us take a basis vector $|\alpha; \lambda(0)\rangle$ at $t = 0$ and study how the state develops as a function of time. We may assume that $\varepsilon(\lambda) = 0$ for any $\lambda \in M$, possibly after first readjusting the

zero-point of the energy. Now our task is to solve the Schrödinger equation

$$i \frac{d}{dt} |\psi_\alpha(t)\rangle = H_{\lambda(t)} |\psi_\alpha(t)\rangle \quad (2)$$

with the initial condition $|\psi_\alpha(0)\rangle = |\alpha; \lambda(0)\rangle$. It follows from the adiabaticity condition that the solution of the above equation may always be expanded in the form

$$|\psi_\alpha(t)\rangle = \sum_{\beta=1}^g |\beta; \lambda(t)\rangle U_{\beta\alpha}(t). \quad (3)$$

The unitarity of the matrix $U_{\beta\alpha}$ follows from the condition $\langle \psi_\beta(t) | \psi_\alpha(t) \rangle = \delta_{\beta\alpha}$. By substituting Eq. (3) into Eq. (2), we find that

$$\dot{U}_{\alpha\beta} = - \sum_{\gamma=1}^g \left\langle \beta; \lambda(t) \left| \frac{d}{dt} \right| \gamma; \lambda(t) \right\rangle U_{\gamma\alpha}. \quad (4)$$

The formal solution of the above equation is readily obtained as

$$\begin{aligned} U(t) &= \mathcal{T} \exp \left(- \int_0^t A(\tau) d\tau \right) \\ &= I - \int_0^t A(\tau) d\tau + \int_0^t d\tau \int_0^\tau d\tau' A(\tau) A(\tau') + \dots \end{aligned} \quad (5)$$

where \mathcal{T} is the time-ordering operator and

$$A_{\beta\alpha}(t) = \left\langle \beta; \lambda(t) \left| \frac{d}{dt} \right| \alpha; \lambda(t) \right\rangle. \quad (6)$$

Let us define the Lie-algebra-valued connection one-form

$$\mathcal{A}_{\beta\alpha} = \left\langle \beta; \lambda(t) \left| \frac{\partial}{\partial \lambda^i} \right| \alpha; \lambda(t) \right\rangle d\lambda^i \quad (7)$$

by which $U(t)$ may be expressed as

$$U(t) = \mathcal{P} \exp \left(- \int_{\lambda(0)}^{\lambda(t)} \mathcal{A} \right), \quad (8)$$

where \mathcal{P} is the path-ordering operator. Note that \mathcal{A} is anti-Hermitian; $\mathcal{A}^\dagger = -\mathcal{A}$.

Suppose that the path $\lambda(t)$ is a loop $\gamma(t)$ ($0 \leq t \leq T$) in M , such that $\gamma(0) = \gamma(T) = \lambda_0$. Then it is found after traversing the loop γ that the resulting state is

$$|\psi_\alpha(T)\rangle = \sum_{\beta=1}^g |\beta; \lambda_0\rangle U_{\beta\alpha}(T). \quad (9)$$

The unitary matrix

$$U_\gamma \equiv U(T) = \mathcal{P} \exp \left(- \oint_\gamma \mathcal{A} \right) \quad (10)$$

is called the holonomy associated with the loop γ . It is clear that U_γ is independent of the parameterization for the loop but only depends on the geometric image of the loop in M .

Suppose the initial state is a superposition

$$|\psi(0)\rangle = \sum_{\alpha=1}^g c_\alpha(\text{in})|\alpha; \lambda_0\rangle.$$

Then the linearity of the Schrödinger equation leads to the final state

$$\begin{aligned} |\psi(T)\rangle &\equiv \sum_{\beta=1}^g c_\beta(\text{out})|\beta; \lambda_0\rangle \\ &= \sum_{\beta=1}^g |\beta; \lambda_0\rangle U_{\beta\alpha}(T) c_\alpha(\text{in}) \end{aligned} \quad (11)$$

which implies that $c_\beta(\text{out}) = \sum_\alpha U_{\beta\alpha}(T) c_\alpha(\text{in})$. Thus, we confirm that U is indeed the matrix representation of the time-evolution operator with the standard ordering of indices. In this context, it is crucial that the summation in Eq. (3) goes over the first index β .

The space of all the loops based at λ_0 is denoted as

$$L_{\lambda_0}(M) = \{\gamma : [0, T] \rightarrow M | \gamma(0) = \gamma(T) = \lambda_0\}. \quad (12)$$

The set of the holonomy

$$\text{Hol}(\mathcal{A}; \lambda_0) = \{U_\gamma | \gamma \in L_{\lambda_0}(M)\} \quad (13)$$

has a group structure and is called the holonomy group. The product is just an ordinary matrix product. It is easily seen that $\text{Hol}(\mathcal{A}; \lambda_0)$ is isomorphic to $\text{Hol}(\mathcal{A}; \lambda_1)$ for any $\lambda_0, \lambda_1 \in M$ if M is arcwise-connected. It is clear that $\text{Hol}(\mathcal{A}) \subset U(g)$ since $U(g)$ is the maximal possible group in \mathbb{C}^g , which preserves the norm of a vector. The connection \mathcal{A} is called irreducible if $\text{Hol}(\mathcal{A}) = U(g)$. We assume that our control manifold is always arcwise-connected and we omit the explicit quotation of the base point from now on.

3. Three-State Model and Quantum-Gate Construction

3.1. One-qubit gates

To realize the idea outlined in the previous section, we employ a simple model Hamiltonian called the three-state model as the basic building block for our strategy. This is a 3-dimensional Hamiltonian defined by

$$H_{\lambda_0} = \epsilon |2\rangle\langle 2| = \begin{pmatrix} \epsilon & 0 & 0 \\ 0 & 0 & 0 \\ 0 & 0 & 0 \end{pmatrix} \quad (14)$$

at the base point $\lambda_0 \in M$. The first column (row) of the matrix refers to the auxiliary state $|2\rangle$ with an energy $\epsilon > 0$ while the second and the third columns (rows) refer to the vectors $|0\rangle$ and $|1\rangle$, respectively, having vanishing energy. The computational subspace (qubit) consists of

the last two vectors. In spite of the fact that the qubit operation takes place in this subspace, the auxiliary state $|2\rangle$ is necessary since the Hamiltonian trivially vanishes otherwise.

The control manifold M of the Hamiltonian (14) is the complex projective space $\mathbb{C}P^2 = U(3)/(U(2) \times U(1))$. This is seen most directly as follows: The most general form of the isospectral deformation of the Hamiltonian is of the form $H_\gamma \equiv W_\gamma H_{\lambda_0} W_\gamma^\dagger$, where $W_\gamma \in U(3)$. Note, however, that not all the elements of $U(3)$ are independent. It is clear that H_γ is independent of the overall phase of W_γ , which reduces the degrees of freedom from $U(3)$ to $U(3)/U(1) \cong SU(3)$. Moreover, any element of $SU(3)$ may be decomposed into a product of three $SU(2)$ matrices as follows

$$W_\gamma = \underbrace{\begin{pmatrix} \bar{\beta}_1 & \bar{\alpha}_1 & 0 \\ -\alpha_1 & \beta_1 & 0 \\ 0 & 0 & 1 \end{pmatrix}}_{U_1} \underbrace{\begin{pmatrix} \bar{\beta}_2 & 0 & \bar{\alpha}_2 \\ 0 & 1 & 0 \\ -\alpha_2 & 0 & \beta_2 \end{pmatrix}}_{U_2} \underbrace{\begin{pmatrix} 1 & 0 & 0 \\ 0 & \bar{\beta}_3 & \bar{\alpha}_3 \\ 0 & -\alpha_3 & \beta_3 \end{pmatrix}}_{U_3}, \quad (15)$$

where the α_j and the β_j satisfy the relation $|\alpha_j|^2 + |\beta_j|^2 = 1$. This decomposition is known as the Givens decomposition. We put $\alpha_j = e^{i\phi_j} \sin \theta_j$ and $\beta_j = e^{i\psi_j} \cos \theta_j$. It is clear that H_γ is independent of U_3 since $U_3 H_{\lambda_0} U_3^\dagger = H_{\lambda_0}$. This further reduces the physical degrees of freedom to $SU(3)/SU(2) \cong S^5$. This is not the end of the story, however, since $\mathbb{C}P^2$ is real four-dimensional and we have to get rid of a phase from S^5 . Accordingly, we have to “gauge away” two redundant parameters in the product $U_1 U_2$ which contains altogether six parameters. These redundancies are easily identified by writing the product out explicitly. The result depends only on the combination $\phi_2 - \psi_2$ and not on individual parameters. Accordingly, we may redefine ϕ_2 as $\phi_2 - \psi_2$ to eliminate ψ_2 . Furthermore, after this redefinition we find that the Hamiltonian depends only on $\phi_1 - \psi_1$ and $\phi_2 - \psi_1$ and hence ψ_1 may also be subsumed by redefining ϕ_1 and ϕ_2 , which reduces the independent degrees of freedom down to $\mathbb{C}P^2 \cong S^5/S^1$.

Let $[z^1, z^2, z^3]$ be the homogeneous coordinate of $\mathbb{C}P^2$ and $(1, \xi_1, \xi_2)$ be the corresponding inhomogeneous coordinate, where $\xi_1 = z^2/z^1, \xi_2 = z^3/z^1$ in the coordinate neighborhood with $z^1 \neq 0$. If we write $\xi_k = r_k e^{i\varphi_k}$ the above correspondence, i.e. the embedding of $\mathbb{C}P^2$ into $U(3)$, is explicitly given by $\theta_k = \tan^{-1} r_k$ and $\phi_k = \varphi_k$.

The connection coefficients are easily calculated in the present model and are given by

$$\mathcal{A}_{\theta_1} = \begin{pmatrix} 0 & -\sin \theta_2 e^{-i(\phi_2 - \phi_1)} \\ \sin \theta_2 e^{i(\phi_2 - \phi_1)} & 0 \end{pmatrix}, \quad (16)$$

$$\mathcal{A}_{\theta_2} = \begin{pmatrix} 0 & 0 \\ 0 & 0 \end{pmatrix}, \quad (17)$$

$$\mathcal{A}_{\phi_1} = \begin{pmatrix} -i \sin^2 \theta_1 & -\frac{i}{2} \sin 2\theta_1 \sin \theta_2 e^{i(\phi_1 - \phi_2)} \\ -\frac{i}{2} \sin 2\theta_1 \sin \theta_2 e^{i(\phi_2 - \phi_1)} & i \sin^2 \theta_2 \sin^2 \theta_1 \end{pmatrix}, \quad (18)$$

$$\mathcal{A}_{\phi_2} = \begin{pmatrix} 0 & 0 \\ 0 & -i \sin^2 \theta_2 \end{pmatrix}, \quad (19)$$

where the first column (row) refers to $|0\rangle$ while the second one refers to $|1\rangle$. Using these connection coefficients, it is possible to evaluate the holonomy associated with a loop γ as

$$U_\gamma = \mathcal{P} \exp \left(- \oint_\gamma (\mathcal{A}_{\theta_1} d\theta_1 + \mathcal{A}_{\theta_2} d\theta_2 + \mathcal{A}_{\phi_1} d\phi_1 + \mathcal{A}_{\phi_2} d\phi_2) \right). \quad (20)$$

Now our task is to find a loop that yields a given unitary matrix as its holonomy.

3.2. Two-qubit gates

Let us next consider a two-qubit reference Hamiltonian

$$H_{\lambda_0}^{2\text{-qubit}} = H_{\lambda_0}^a \otimes I_3 + I_3 \otimes H_{\lambda_0}^b, \quad (21)$$

where $H_\lambda^{a,b}$ are three-state Hamiltonians and I_3 is the 3×3 unit matrix. Generalization to an arbitrary N -qubit system is obvious. The Hamiltonian scales as 3^N , instead of the 2^N in the present model.

We want to preserve the multipartite structure of the system in constructing the holonomy. For this purpose, we separate the unitary transformation into a tensor product of single-qubit transformations ($W_\gamma^a \otimes W_\gamma^b$) and a purely two-qubit rotation $W_\gamma^{2\text{-qubit}}$ which cannot be reduced into a tensor product of single-qubit transformations. Therefore, we write the isospectral deformation for a given loop γ as

$$H_\gamma^{2\text{-qubit}} = W_\gamma^{2\text{-qubit}} (W_\gamma^a \otimes W_\gamma^b) H_{\lambda_0}^{2\text{-qubit}} (W_\gamma^a \otimes W_\gamma^b)^\dagger W_\gamma^{2\text{-qubit}\dagger}. \quad (22)$$

The advantage of expressing the unitary matrix in this form is easily verified when we write down the connection coefficients for the one-qubit coordinates. Namely, the two-qubit transformation does not affect the one-qubit transformation at all;

$$\begin{aligned} \mathcal{A}_{i,\alpha\beta} &= \left\langle \alpha; \lambda \left| W_\gamma^\dagger \frac{\partial}{\partial \gamma^i} W_\gamma \right| \beta; \lambda \right\rangle \\ &= \left\langle \alpha; \lambda \left| (W_\gamma^a \otimes W_\gamma^b)^\dagger \frac{\partial}{\partial \gamma^i} (W_\gamma^a \otimes W_\gamma^b) \right| \beta; \lambda \right\rangle, \end{aligned}$$

where γ^i denotes a one-qubit coordinate.

There is a large number of possible choices for $W_\gamma^{2\text{-qubit}}$, depending on the physical realization of the present scenario. To keep our analysis as concrete as possible, we have made the simplest choice

$$W_\gamma^{2\text{-qubit}} = W_\xi \equiv e^{i\xi|11\rangle\langle 11|} \quad (23)$$

for our two-qubit unitary rotation. Let

$$\begin{aligned} H'_\gamma &= H_\gamma^a \otimes I_3 + I_3 \otimes H_\gamma^b \\ &= \begin{pmatrix} h_{11}^a + h_{11}^b & h_{12}^b & h_{13}^b & h_{12}^a & 0 & 0 & h_{13}^a & 0 & 0 \\ h_{21}^b & h_{11}^a + h_{22}^b & h_{23}^b & 0 & h_{12}^a & 0 & 0 & h_{13}^a & 0 \\ h_{31}^b & h_{32}^b & h_{11}^a + h_{33}^b & 0 & 0 & h_{12}^a & 0 & 0 & h_{13}^b \\ h_{21}^a & 0 & 0 & h_{22}^a + h_{11}^b & h_{12}^b & h_{13}^b & h_{23}^a & 0 & 0 \\ 0 & h_{21}^a & 0 & h_{21}^b & h_{22}^a + h_{22}^b & h_{23}^b & 0 & h_{23}^a & 0 \\ 0 & 0 & h_{21}^a & h_{31}^b & h_{32}^b & h_{22}^a + h_{33}^b & 0 & 0 & h_{23}^a \\ h_{31}^a & 0 & 0 & h_{32}^a & 0 & 0 & h_{33}^a + h_{11}^b & h_{12}^b & h_{13}^b \\ 0 & h_{31}^a & 0 & 0 & h_{32}^a & 0 & h_{21}^b & h_{33}^a + h_{22}^b & h_{23}^b \\ 0 & 0 & h_{31}^a & 0 & 0 & h_{32}^a & h_{31}^b & h_{32}^b & h_{33}^a + h_{33}^b \end{pmatrix}. \end{aligned}$$

be a two-qubit Hamiltonian before W_ξ is applied. Then after the application of W_ξ to H'_γ we obtain for the full Hamiltonian

$$\begin{aligned}
H_\gamma^{2\text{-qubit}} &= W_\xi H'_\gamma W_\xi^\dagger \\
&= \begin{pmatrix}
h_{11}^a + h_{11}^b & h_{12}^b & h_{13}^b & h_{12}^a & 0 & 0 & h_{13}^a & 0 & 0 \\
h_{21}^b & h_{11}^a + h_{22}^b & h_{23}^b & 0 & h_{12}^a & 0 & 0 & h_{13}^a & 0 \\
h_{31}^b & h_{32}^b & h_{11}^a + h_{33}^b & 0 & 0 & h_{12}^a & h_{13}^a & 0 & h_{13}^b e^{-i\xi} \\
h_{21}^a & 0 & 0 & h_{22}^a + h_{11}^b & h_{12}^b & h_{13}^b & h_{23}^a & 0 & 0 \\
0 & h_{21}^a & 0 & h_{21}^b & h_{22}^a + h_{22}^b & h_{23}^b & 0 & h_{23}^a & 0 \\
0 & 0 & h_{21}^a & h_{31}^b & h_{32}^b & h_{22}^a + h_{33}^b & 0 & 0 & h_{23}^a e^{-i\xi} \\
h_{31}^a & 0 & 0 & h_{32}^a & 0 & 0 & h_{33}^a + h_{11}^b & h_{12}^b & h_{13}^b e^{-i\xi} \\
0 & h_{31}^a & 0 & 0 & h_{32}^a & 0 & h_{21}^b & h_{33}^a + h_{22}^b & h_{23}^b e^{-i\xi} \\
0 & 0 & h_{31}^a e^{i\xi} & 0 & 0 & h_{32}^a e^{i\xi} & h_{31}^b e^{i\xi} & h_{32}^b e^{i\xi} & h_{33}^a + h_{33}^b
\end{pmatrix}. \tag{24}
\end{aligned}$$

As for the connection, we find

$$\mathcal{A}_\xi = \begin{pmatrix} 0 & 0 & 0 & 0 \\ 0 & 0 & 0 & 0 \\ 0 & 0 & 0 & 0 \\ 0 & 0 & 0 & i \cos^2 \theta_2^a \cos^2 \theta_2^b \end{pmatrix} \tag{25}$$

where the rows and columns are ordered with respect to the basis $\{|00\rangle, |01\rangle, |10\rangle, |11\rangle\}$. It should be apparent from the above analysis that we can construct an arbitrary controlled phase-shift gate with the help of a loop in the (θ_2^a, ξ) - or (θ_2^b, ξ) -space. Accordingly, this yields the CNOT gate with one-qubit operations, as shown below.

3.3. Some Examples

Prior to proceeding to present in the next section the numerical prescription to construct arbitrary one- and two-qubit gates, it is instructive to first work out some important examples whose loop can be constructed analytically. In particular, we will show that all the gates required for the proof of universality may be obtained within the present three-state model.

The first example is the $\pi/8$ -gate,

$$U_{\pi/8} = \begin{pmatrix} 1 & 0 \\ 0 & e^{i\pi/8} \end{pmatrix}. \tag{26}$$

By inspecting the connection coefficients in Eqs. (16–19), we easily find that the loop

$$(\theta_2, \phi_2) : (0, 0) \rightarrow (\pi/2, 0) \rightarrow (\pi/2, \pi/8) \rightarrow (0, \pi/8) \rightarrow (0, 0). \tag{27}$$

yields the desired gate. Note that the loop is in the (θ_2, ϕ_2) -plane and that all the other parameters are fixed at zero. Explicitly, we verify that

$$\begin{aligned}
U_{\pi/8} &= \exp\left(\frac{\pi}{8} \mathcal{A}_{\phi_2}|_{\theta_2=0}\right) \exp\left(\frac{\pi}{2} \mathcal{A}_{\theta_2}|_{\phi_2=\pi/8}\right) \\
&\quad \times \exp\left(-\frac{\pi}{8} \mathcal{A}_{\phi_2}|_{\theta_2=\pi/2}\right) \exp\left(-\frac{\pi}{2} \mathcal{A}_{\theta_2}|_{\phi_2=0}\right) \\
&= \exp\left(-\frac{\pi}{8} \mathcal{A}_{\phi_2}|_{\theta_2=\pi/2}\right). \tag{28}
\end{aligned}$$

The next example is the Hadamard gate

$$H = \frac{1}{\sqrt{2}} \begin{pmatrix} 1 & 1 \\ 1 & -1 \end{pmatrix}. \quad (29)$$

Instead of constructing H directly, we will rather choose to use the decomposition

$$H = e^{-i\pi/2} \exp\left(i\frac{\pi}{2}\sigma_z\right) \exp\left(i\frac{\pi}{4}\sigma_y\right).$$

It is easy to verify that the holonomy associated with the loop

$$(\theta_2, \theta_1) : (0, 0) \rightarrow (\pi/2, 0) \rightarrow (\pi/2, \beta) \rightarrow (0, \beta) \rightarrow (0, 0) \quad (30)$$

is $\exp(i\beta\sigma_y)$, while that associated with the loop

$$\begin{aligned} (\theta_1, \theta_2, \phi_1) : (0, 0, 0) &\rightarrow (\pi/2, 0, 0) \rightarrow (\pi/2, \pi/2, 0) \rightarrow (\pi/2, \pi/2, \alpha) \\ &\rightarrow (\pi/2, 0, \alpha) \rightarrow (0, 0, \alpha) \rightarrow (0, 0, 0) \end{aligned} \quad (31)$$

is $\exp(i\alpha\sigma_z)$. Here again, the rest of the parameters are fixed at zero. Finally, we construct the phase-shift gate $e^{i\delta}$, which is produced by a sequence of two loops. First we construct a gate similar to the δ -shift gate using (cf., the $\pi/8$ -shift gate)

$$(\theta_1, \phi_1) : (0, 0) \rightarrow (\pi/2, 0) \rightarrow (\pi/2, \delta) \rightarrow (0, \delta) \rightarrow (0, 0). \quad (32)$$

This loop followed by the similar loop in the (θ_2, ϕ_2) -space yields the $e^{i\delta}$ -gate as

$$\begin{aligned} (\theta_1, \phi_1, \theta_2, \phi_2) : (0, 0, 0, 0) &\rightarrow (0, 0, \pi/2, 0) \rightarrow (0, 0, \pi/2, \delta) \rightarrow (0, 0, 0, \delta) \\ &\rightarrow (0, 0, 0, 0) \rightarrow (\pi/2, 0, 0, 0) \rightarrow (\pi/2, \delta, 0, 0) \rightarrow (0, \delta, 0, 0) \rightarrow (0, 0, 0, 0). \end{aligned} \quad (33)$$

Finally, the controlled-phase gate $U(\Theta) = \exp(i\Theta|11\rangle\langle 11|)$ can be implemented with the loop

$$(\theta_2^a, \xi) : (0, 0) \rightarrow (\pi/2, 0) \rightarrow (\pi/2, \Theta) \rightarrow (0, \Theta) \rightarrow (0, 0). \quad (34)$$

4. Numerical Results

4.1. Loop-Finding Algorithm

In this Section we numerically study the construction of holonomic quantum gates for the three-state model. The three-state model is in a way the simplest possible model for holonomic quantum computing while still maintaining the tensor-product structure which is necessary for exponential speed-up. We have previously shown [10] how to solve the inverse problem of finding loops corresponding to desired quantum-logic gates. We have presented several example solutions for various one- and two-qubit gates. We demonstrated, e.g., how to construct the Hadamard gate, the CNOT, the SWAP, and the two-qubit Fourier transform in a single loop. We concluded that our three-state model is capable of universal quantum computing.

Here we will extend the scenario by adding a penalty term for the length of the path. We will also introduce and test a method for optimizing with respect to the length directly but

with a penalty term arising due to excess deviation from the desired gate. In this manner one may efficiently combine loops. Even though these measures will not result in a change in the quantum-computational complexity, it may be possible to significantly reduce the multipliers in front of the highest-order terms in the expression for the CPU execution time. In other words, the big-O notation is the same, but nevertheless, much of the computation time may be saved.

First we review our basic algorithm and show some new example gates. Namely, each loop γ in the parameter space corresponds to a gate U_γ . We wish to solve the inverse problem; We look for a $\hat{\gamma}$ that corresponds to \hat{U} . We further restrict ourselves to the space of all polygonal loops. If \mathcal{V} is the space of all possible loops with the given base point, then \mathcal{V}_k will be the space of all those polygonal loops that have k vertices in addition to the base point. Here of course $\mathcal{V}_k \subset \mathcal{V}$. This problem can be formulated as an optimization problem. One needs to find $\hat{\gamma}$ such that

$$f(\gamma) = \|\hat{U} - U_\gamma\|_F \tag{35}$$

is minimized over all $\gamma \in \mathcal{V}_k$. We aim at the minimum value to be zero. Here $\|\cdot\|_F$ denotes the Frobenius norm defined as $\|A\|_F = \sqrt{\text{Tr}(A^\dagger A)}$.

For one-qubit gates, the dimension is $4k$ whereas in the case of two-qubit gates the dimension is $9k$. We used the polytope algorithm [15] to solve this problem. The reason for employing this method is the extremely complicated structure of the objective function. In Fig. 1 we have plotted a 2D section of the function values. This figure was obtained by using the line joining two known minima of a certain one-qubit gate along with a randomly chosen perpendicular direction. Thus derivative-based methods are not expected to perform well.

The calculation of the holonomy requires evaluating the ordered product in Eq. (10). The method used in the numerical algorithm is to simply write the ordered product in a finite-difference approximation by considering the connection components as being constant over a small difference in the parameters $\delta\gamma_i$.

For instance, we attempted to find a loop corresponding to the Hadamard gate. We have previously given a different implementation of this gate [10]. The resulting loop is illustrated in Fig. 2. Note that this optimization was carried out in \mathcal{V}_3 meaning that there are three vertices other than the reference point. We have taken the origin to be this reference point. The length of this example loop is 12.01 in the Euclidean approximation. To give an example of a two-qubit gate, we have included in Fig. 3 a loop that yields the well-known two-qubit quantum version of the Fourier transform. This loop is again different from the example solutions of Ref. [10]. Thus one is convinced that the solution is by no means unique. For instance, the solution depends strongly on the initial configuration of the polytope algorithm. Hence, there is ample motivation to search for shorter loops.

To show more clearly the power of our technique, we have plotted in Fig. 4 the error as a function of function evaluations for three independent runs. The attempted logical operation was the Hadamard gate. We see that the convergence seems to be exponential. Moreover, a few hundred evaluations of $f(\gamma)$ is enough to achieve an error as low as 10^{-8} . We argue that one can achieve arbitrarily small errors by running the algorithm long enough. Numerical rounding errors will, though, complicate things slightly. It is important from the experimental point of view just to achieve low enough errors.

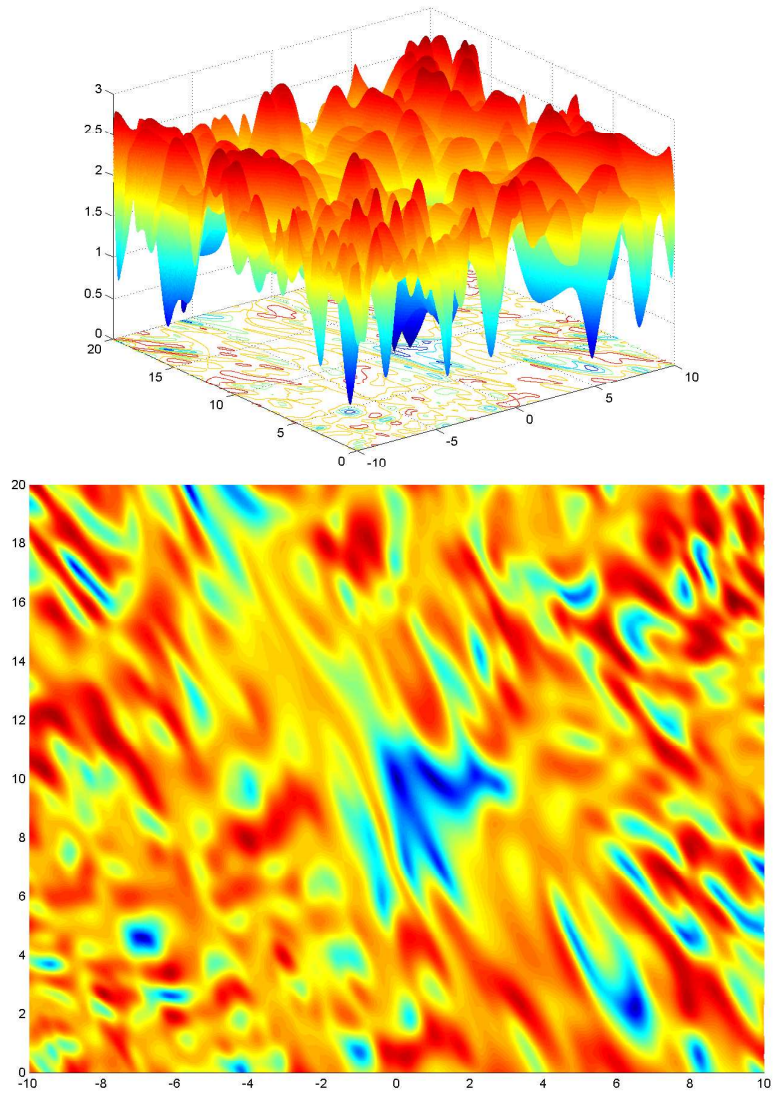


Fig. 1. 2D cross-section of the 12-dimensional objective function.

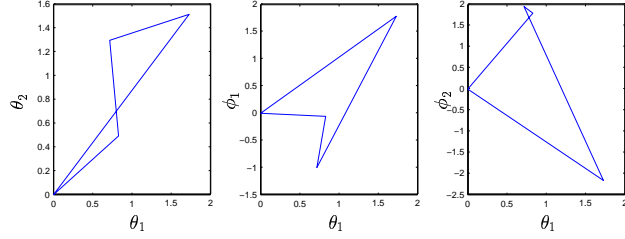


Fig. 2. Loop in the parameter space that implements the Hadamard gate with $L(\gamma_H) = 12.01$.

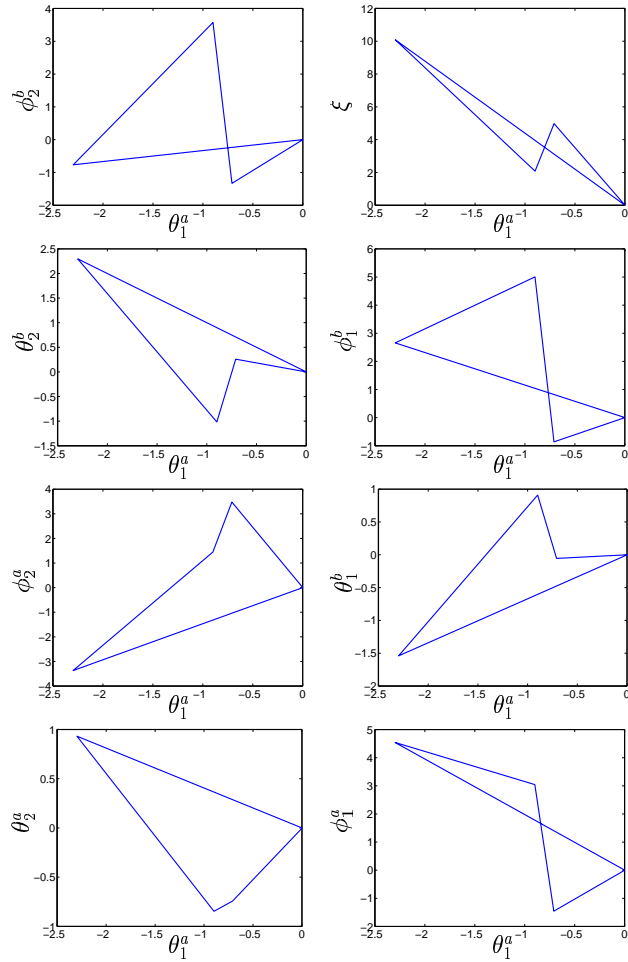


Fig. 3. Loop γ_{Fourier} in the parameter space that gives the two-qubit Fourier gate. Here $L(\gamma_{\text{Fourier}}) = 63.35$. The error was below 10^{-13} .

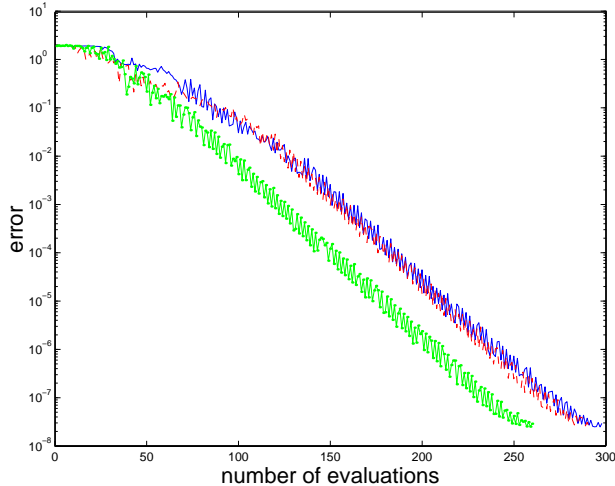


Fig. 4. Error as a function of iterations for the Hadamard gate.

4.2. Length-Penalty Optimization

We now proceed to develop the formalism for reducing the length of the loops. We tried adding a penalty term to the objective function see, e.g., Ref. [14]. This function is defined as

$$P(\gamma) = \begin{cases} 0, & \text{if } L(\gamma) < L_{\max} \\ \nu L(\gamma)^p, & \text{otherwise} \end{cases} \quad (36)$$

where $L(\gamma)$ is the length of the path γ ; here p and ν are adjustable parameters. Note that the length need not be Euclidean. Our numerical experiments below will, though, use the Euclidean approximation. To be strict, however, we would have to relate the four parameters of our Givens decomposition to the base manifold $\mathbb{C}P^2$ of the bundle $U(3)$ in the case of one-qubit gates. Then we would employ the $\mathbb{C}P^2$ metric to evaluate the length of the loop in the optimization algorithm. Hence the lengths of the loops here should be interpreted with caution. Moreover, since HQC is purely geometrical, the operation should be independent of how fast the loop is traversed. Note, however, that a shorter loop may be traversed more quickly without spoiling the adiabaticity requirement.

It should be clear from the structure of Eq. (36) that the penalty functions are designed to have built-in constraints. In the allowed region, i.e., where the length does not exceed L_{\max} , the problem is unchanged. There will be a rapidly growing penalty term elsewhere. From the point of view of the optimization algorithm, short loops are preferred.

Figure 5 illustrates another example solution to the problem of finding a two-qubit Fourier gate but this time with the restriction $L_{\max} = 40$. We have chosen a penalty function with the parameters $p = 2$ and $\nu = 1000$. The solution tends to be on the surface $L(\gamma) = L_{\max}$, at least for short L_{\max} . This may be interpreted to originate from the scarcity of the minima for short loops. Tests show that adjusting the maximum length upwards does not result in a solution

very near to the boundary but rather a solution is found in the middle of the volume. One is inclined to deduce from all this that the number of solutions to the minimization problem is huge. This particular loop is shorter than our earlier construction, but not much. However, our first example in Fig. 3 had a loop length of 63.35, such that a remarkable improvement has been achieved.

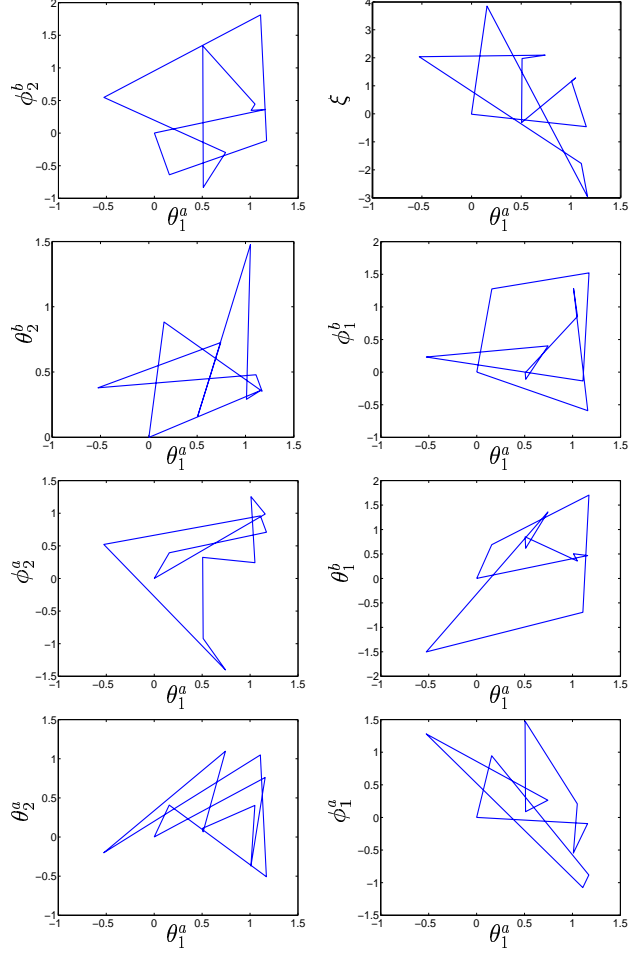


Fig. 5. Length-optimized loop for the quantum Fourier transform in \mathcal{V}_{10} . Here $L(\gamma_{\text{Fourier}}) \approx 39.96$ and the error is below 10^{-13} with 200 discretization points per edge.

A more impressive reduction of length may be seen in Fig. 6. We have previously shown [10] an implementation of the SWAP gate that had a length of 107.85. The gate given below has a length of just 29.99. We managed to cut off a major redundant portion of the path.

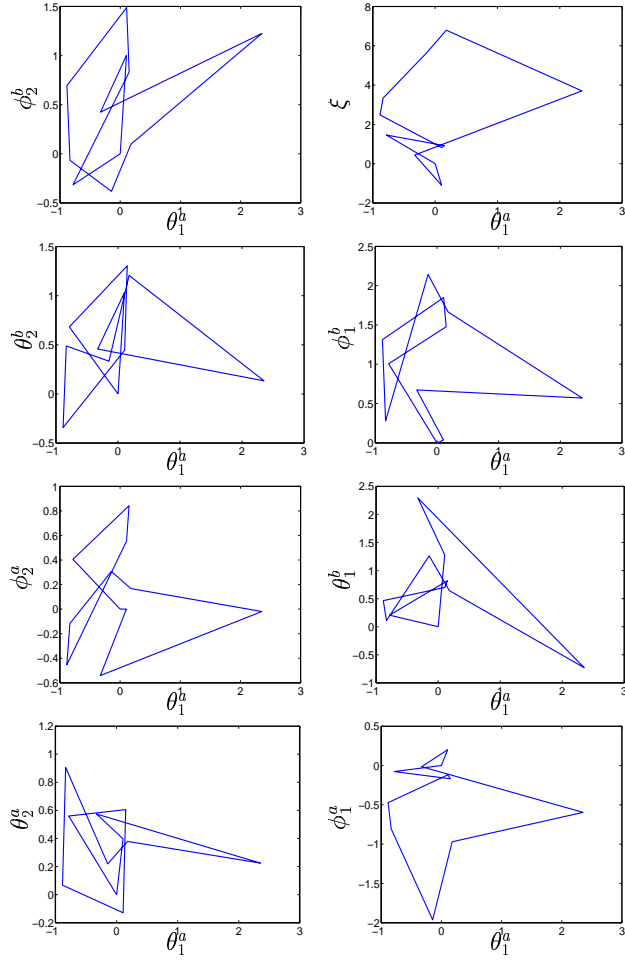


Fig. 6. Length-optimized loop for SWAP in \mathcal{V}_{10} . Here $L(\gamma_{\text{SWAP}}) \approx 29.99$ and the error is below 10^{-13} with 200 discretization points per edge. The loop presented in Ref. [10] had a length of 107.85.

4.3. Error-Penalty Optimization

We can take the concept of length-penalty optimization one step further. Once we know some loop that produces the desired gate, we may switch the roles of the length of the loop and that of the error. Namely, we assign a penalty function that penalizes for excess error while the main contribution comes from the length. In this manner we can try to make increasingly improved loops that yield the very same quantum gate. That is, we minimize the function

$$F(\gamma) = L(\gamma) + P_2(\gamma) \quad (37)$$

where the penalty term is this time given by

$$P_2(\gamma) = \begin{cases} 0, & \text{if } f(\gamma) < \varepsilon_{\max} \\ \nu f(\gamma)^p, & \text{otherwise.} \end{cases} \quad (38)$$

Here $f(\gamma)$ is the error just as previously. This elaboration of the penalty-function technique proves quite powerful.

A good example of the technique is given by the CNOT gate which we may easily perform analytically. We take an implementation of the CNOT

$$\begin{aligned} (\theta_2^a, \theta_2^b, \theta_1^b, \xi) = (0, 0, 0, 0) & \rightarrow (0, \pi/2, 0, 0) & \rightarrow (0, \pi/2, \pi/4, 0) & \rightarrow \\ (0, 0, \pi/4, 0) & \rightarrow (0, 0, 0, 0) & \rightarrow (\pi/2, 0, 0, 0) & \rightarrow \\ (\pi/2, 0, 0, \pi) & \rightarrow (0, 0, 0, \pi) & \rightarrow (0, 0, 0, 0) & \rightarrow \\ (0, \pi/2, 0, 0) & \rightarrow (0, \pi/2, -\pi/4, 0) & \rightarrow (0, 0, -\pi/4, 0) & \rightarrow \\ (0, 0, 0, 0). & & & \end{aligned} \quad (39)$$

as the initial guess of the optimization task where the vertices are joined linearly. This loop is naturally in \mathcal{V}_{11} but we also add an extra vertex in the middle of each edge such that the loop is more flexible and therefore belongs to \mathcal{V}_{23} . The resulting loop after error-penalty minimization is shown in Fig. 7. This figure, as well as all the figures in this section, was obtained by first using poor accuracy and then by minimizing further with improving accuracy starting from the initial guess thus obtained. The starting length was 18.8496 and as can be seen from the length of this loop 14.03, the solution has improved considerably. This is just one example of the power of our technique. Due to the success of the method we are yet more convinced that the acceptable solutions are extremely dense in parameter space.

The use of the Euclidean metric is particularly well motivated in the context of error-penalty optimization. Of course, the underlying physical setting might suggest using a specialized metric that would relate some experimental ‘‘cost’’ to certain areas of the base manifold. For example, it is not clear which shape of the manifold one should choose, analogously to the situation between ellipsoids and spheres. In the present scenario we have two objectives: a low error and a short path. If there emerges a redundant contribution adding to the length from some part of the manifold where the parameterization is not one-to-one, this excess length can be removed without affecting the solution. Since we are also aiming at reducing the Euclidean length, any redundant contributions tend to disappear in practice due to the minimization algorithm. An analogy is provided by the unit ball S^2 ; if one were to do a

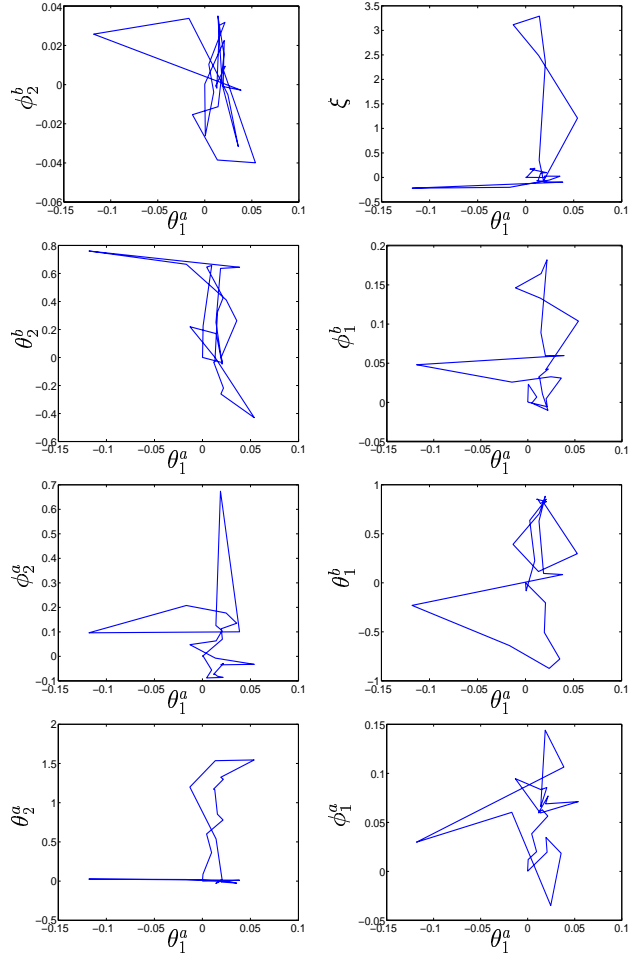


Fig. 7. Result of the error-penalty minimization of an initially known CNOT loop in \mathcal{V}_{23} . Here $L(\gamma_{\text{CNOT}}) \approx 14.03$. The original loop was in \mathcal{V}_{11} , had a length of 18.85 and actually consisted of three individual loops.

2π turn on one of the poles, there would be an Euclidean contribution that would have no meaning. This excess length would disappear in the minimization process, though.

5. Discussion

We have numerically studied the construction of holonomic quantum gates. Our method is capable of finding the loop in the parameter space corresponding to any one- or two-qubit gate in a three-state model. It seems reasonable that the method would also work in other models. The optimization task is too difficult for derivative-based methods as can be seen in the pictures we have presented. The polytope algorithm has, however, proved useful in this task. Moreover, our previous calculations prove the three-state model that we have presented capable of universal HQC. We discussed example solutions for the Hadamard gate and the two-qubit Fourier transform without length considerations. It is easy to construct a set of universal gates for the model analytically. Numerical results are, though, far superior since they realize a given unitary matrix with a shorter single loop.

In the present paper we have developed a method for minimizing with respect to the length of the loop, thus making the implementation of these holonomies as quick as possible. We have first investigated adding a penalty term for excess length and then experimented swapping the roles of the length and the error. Provided that one already knows some implementation of a desired gate, this latter technique can be used to combine loops in an efficient manner. The results that we have obtained appear promising. The main result is that the optimization problem can be solved even though the landscape is quite rough. For one- and two-qubit gates a regular PC suffices.

It must be emphasized that it certainly is desirable for the loop to have the shortest possible length to achieve fast operation speed without sacrificing the adiabaticity. As a preliminary to our optimization scheme, we neglected the underlying metric of $\mathbb{C}P^2 \simeq U(3)/U(2) \times U(1)$ and pretended as if we were working in a manifold with an Euclidean metric. We demonstrated that our scheme works reliably. We are currently engaged in a more ambitious program with the $\mathbb{C}P^2$ metric properly taken into account. We believe that our optimization method could also be extended to more conventional quantum-computing schemes. Then, however, time would appear explicitly in the minimization.

A few remarks are in order about our method. The fact that the optimization landscape is rough does not imply that HQC would be sensitive to errors. Namely, physical errors do not just move one vertex but rather there are deviations all along the path. To which degree this causes errors would constitute a separate study. Furthermore, increasing the number of vertices does not result in an improved accuracy: For one-qubit gates it is enough to have $2^2 = 4$ independent parameters and for two-qubit gates $4^2 = 16$ parameters. This is because $U(2^N)$ is parameterized by 2^{2N} real parameters. Recall that the number of optimization variables is either $4k$ or $9k$. With $k = 1$ one cannot, however, obtain a non-trivial holonomy. More vertices might mean less length, though.

The speed-up must be considered in terms of the adiabatic time. Short loops can always be traversed slowly but they may also be traversed more quickly. It is important to reduce the operation time to fight the effect of decoherence. Thus the optimization of quantum gates is a very well motivated task.

We wish to point out that all the rotations in $\mathbb{C}P^2$ are available with a construction using

superconducting nanostructures [17].

Acknowledgments

AON would like to thank the Research Foundation of Helsinki University of Technology and the Graduate School in Technical Physics for financial support; MN thanks the Helsinki University of Technology for a Visiting Professorship and he is also grateful for partial support of Grant-in-Aid from the Ministry of Education, Culture, Sports, Science, and Technology, Japan (Project Nos. 14540346 and 13135215); MMS acknowledges the Academy of Finland for a Research Grant in Theoretical Materials Physics.

Note added in proof: It was brought to our attention that the minimization of the loop length for a given holonomy has become known as the "isoholonomic problem", named in analogy with the "isoperimetric problem" in which the area surrounded by a loop with fixed length is maximized. See, e.g., R. Montgomery, "Isoholonomic problems and some applications", Commun. Math. Phys. **128**, 565–592 (1990). In Montgomery's paper, this minimization problem is written in the form of a differential equation. In our approach, however, this does not work since there occur too many local minima. Therefore, we consider our minimization algorithm a far more practical scheme.

References

1. P. Zanardi and M. Rasetti, *Holonomic quantum computation*, Phys. Lett. A **264**, 94-99, 1999.
2. K. Fujii, *Mathematical foundations of holonomic quantum computer*, Rep. Math. Phys. **48**, 75-82, 2001.
3. J. Pachos and S. Chountasis, *Optical holonomic quantum computer*, Phys. Rev. A **62**, 052318, 2000.
4. D. Ellinas and J. Pachos, *Universal quantum computation by holonomic and nonlocal gates with imperfections*, Phys. Rev. A **64**, 022310, 2001.
5. J. Pachos, P. Zanardi and M. Rasetti, *Non-Abelian Berry connections for quantum computation*, Phys. Rev. A **61**, 010305(R), 1999.
6. J. Pachos, P. Zanardi, *Quantum holonomies for quantum computing*, Int. J. Mod. Phys. B **15**, 1257-1285, 2001.
7. M.-S. Choi, *Geometric Quantum Computation on Solid-State Qubits*, LANL e-print, quant-ph/0111019, 2001.
8. L. Faoro, J. Siewert and R. Fazio *Non-Abelian phases, pumping and quantum computation with Josephson Qubits*, LANL e-print, cond-mat/0202217, 2002.
9. M. Berry, *Quantal phase factors accompanying adiabatic changes*, Proc. R. Soc. Lond. A **392**, 45-57, 1984.
10. A. O. Niskanen, M. Nakahara, and M. M. Salomaa, *Realization of arbitrary gates in holonomic quantum computation*, Phys. Rev. A, in print (2002); quant-ph/0209015.
11. F. Wilczek and A. Zee, *Appearance of gauge structure in Simple Dynamical Systems*, Phys. Rev. Lett. **52**, 2111-2114, 1984.
12. A. Zee, *Non-Abelian gauge structure in nuclear quadrupole resonance*, Phys. Rev. A **38**, 1-6, 1988.
13. A. Mostafazadeh, *Generalized Adiabatic Product Expansion: A nonperturbative method of solving time-dependent Schroedinger equation*, J. Math. Phys. **40**, 3311-3326, 1999.
14. M. S. Bazaraa, H. D. Sherali, C. M. Shetty, *Nonlinear Programming, Theory and Algorithms*, John Wiley and Sons, 1993.
15. <http://pangea.stanford.edu/~baris/professional/theorypolytope.html>
16. M. Nakahara, *Geometry, Topology and Physics*, IOP Publishing Ltd., 1990.
17. A. O. Niskanen, M. Nakahara, and M. M. Salomaa, to be published.